Onion-like nanoparticles with γ-Fe core surrounded by a α-Fe/Fe-oxide double shell

M.P. Fernández-García [a,*], P. Gorria [a], M. Sevilla [b], A.B. Fuertes [b], J.M. Grenèche [c], J.A. Blanco [a]

[a] Departamento de Física, Universidad de Oviedo, Calvo Sotelo, s/n, 33007 Oviedo, Spain
[b] Instituto Nacional del Carbón, Apartado 73, 33080 Oviedo, Spain
[c] LPEC, UMR CNRS-6087, Université du Maine, Le Mans, France

ARTICLE INFO

ABSTRACT

Using a low cost and simple chemical procedure, randomly dispersed iron nanoparticles (NPs) embedded in an activated carbon matrix were synthesized. The Fe-NPs exhibit an onion-like morphology that consists on a γ-Fe core surrounded by a double α-Fe (inner)/γ-Fe_2O_3 (outer) shells. The room temperature saturation magnetization value of the Fe-NPs is lower than that of bulk α-Fe as a consequence of the disordered interfacial spins. In addition, the broadening of the low temperature Mössbauer singlet contribution of the γ-Fe phase, seems to suggest a possible magnetic ordering of the core.

© 2011 Elsevier B.V. All rights reserved.

1. Introduction

Magnetic nanoparticles (MNPs) have attracted enormous interest during the last decade due to their technological and biomedical potential applications [1–3]. They are also eye-catching from the fundamental point of view, to tackle the magnetism at the nanoscale and, the influence of either the large surface-to-volume ratio and/or the nature of the matrix on the physical–chemical properties [3,4].

Previous studies on Ni NPs and Co-NPs inserted in an activated carbon (AC) matrix revealed that the synthesis strategy with sucrose mostly influences the final NP morphology, and therefore, their magnetic behaviour [5–7]. In the case of Fe@AC NPs, ferromagnetic (FM) Fe-NPs and ferrimagnetic (FIM) Fe-oxides, successfully synthesized within different protecting coatings and/or matrices, have been largely studied ([1–3,8–11] and references therein). However, γ-Fe NPs have received less attention [10,12–14]. The main reason for that is the difficulty for stabilizing the high temperature (above 1180 K) stable phase of iron, γ-Fe, with face-centered cubic (FCC) crystal structure. However, the study of the γ-Fe magnetism is still an active and fascinating field of research [15,16], where the Fe–Fe next-neighbour interatomic distances play a major role for the existence of FM (high spin) or AFM (low spin) magnetic interactions, being the crossover distance ≈2.54 Å.

We have previously reported the controlled formation of γ-Fe NP cores inside an AC matrix, following a chemical procedure (based on a pyrolysis process at 900 °C) which takes place at the reduced intersections between the nanopores [17,18]. The analysis of the diameter of more than 1500 Fe-NPs on TEM images, reveals a broad single distribution of NP sizes described by a log-normal function centered at $\langle \tau(\mu) \rangle$ 15(6) nm. The Fe-NPs exhibit almost spherical sizes and are randomly distributed on the carbon matrix, displaying onion-like morphologies that consists of: γ-Fe cores with diameters of ∼10(2) nm and a double α-Fe [1.8(5) nm]/γ-Fe_2O_3 [0.8(5) nm] shell (TEM images can be found elsewhere [17–19]). The identification and quantification of the different Fe phases (especially the iron oxide) was only possible by combining room temperature X-ray absorption (XAS) and Mössbauer spectroscopies.

Moreover, a low-temperature exchange bias effect (EB) is observed below 50 K, due to the magnetic coupling between the FIM maghemite ($T_N \sim 1020$ K) and the FM α-Fe shell [19]. Herein we report the analysis of (i) the first quadrant of the magnetization curves, $M(H)$, in order to estimate the saturation magnetization

* Corresponding author.
E-mail address: fernandezpaz.uo@uniovi.es (M.P. Fernández-García).

value, M_s, of the nano-onion NPs, as well as (ii) the Mössbauer spectra recorded at three different temperatures with the aim of obtaining further information about the low temperature magnetic ordering of the γ-Fe phase.

2. Experimental details

The Fe-based nanocomposites were synthesized using a commercial activated porous carbon (AC) as a starting material with mesopores of ~6–7 nm on diameter. The fabrication process is based on a pyrolysis process taking place inside the restricted interconnected porosity of the AC. The pores of the AC matrix were filled with a solution of iron nitrate in ethanol up to incipient wetness. Then, the composite was heat-treated up to 1173 K under N_2 atmosphere and maintained at this temperature for 3 h. On the cooling process the as-prepared sample was stabilized with a small stream of air. The final Fe content of the sample determined by thermogravimetric analysis was estimated to be 16.8 wt.% Fe. Further details are given elsewhere [19].

The $M(H)$ curves were measured on a Quantum Design PPMS-14T equipment with a vibrating sample magnetometer (VSM) option in the range ±20 kOe and at selected temperatures between 60 and 300 K.

The Mössbauer spectra were measured at 4.2, 77 and 300 K in transmission geometry with a conventional constant acceleration spectrometer using a ^{57}Co/Rh source and a standard α-Fe foil for calibration.

3. Results

3.1. Saturation magnetization

The low temperature $M(H)$ curves reveal that the magnetic moment is not saturated even at 20 kOe, indicating a magnetically disordered state of the oxide shell [19,20]. Thus, a careful study of the $M(H)$ curves is needed if an accurate estimation of the saturation magnetization, M_s, of the Fe-NPs is pursued. Fig. 1 displays the $M(H)$ dependence for $H \geq 7.5$ kOe and $T > 50$ K together with a fit to a the law of approach-to-saturation given by the following equation (Eq. (1)):

$$M = M_s \left(1 - \frac{b}{H^2}\right) + \chi_o H \qquad (1)$$

where M_s is the saturation magnetization at each temperature and χ_o is the magnetic susceptibility (see Ref. [21]).

The obtained saturation magnetization vs. temperature, $M_s(T)$, dependence typically follows a Bloch $T^{3/2}$-law for infinitely large systems (bulk) and low temperatures [22]. However, for a model of spin-wave excitations [23], the $M_s(T)$ dependence of particles with BCC and FCC crystal structures is expected to behave as:

$$M_s(T) = M_s(0)(1 - BT^\alpha) \qquad (2)$$

In this power-law equation, $M_s(0)$ is the saturation magnetization at 0 K. For $T > 50$ K, $M_s(T)$ values of Fe-AC composite follows Eq. (2) with an exponent $\alpha = 1.9$, a prefactor $B = 1.4 \times 10^{-6}$ K$^{-1.9}$ and $M_s(0) \sim 13.3$ emu/g (see inset in Fig. 1). The saturation magnetization decreases faster with increasing temperature than in the case
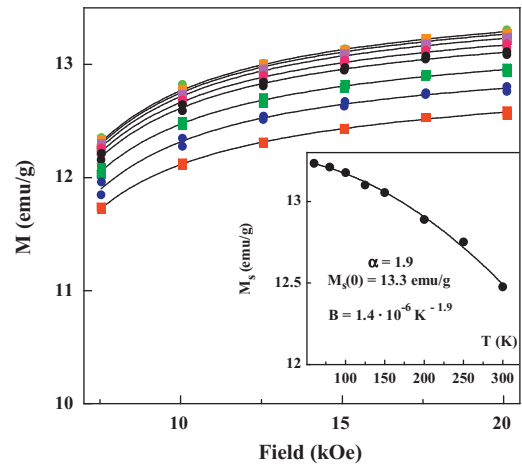

Fig. 1. Magnetization vs. applied magnetic field at 300 K (■), 250 K (●), 200 K (■), 150 K (●), 125 K (●), 100 K (■), 80 K (■) and 60 K (●). The solid line corresponds to the fit following Eq. (1) for $H \geq 7.5$ kOe. The inset shows the temperature dependence of M_s obtained from the $M(H)$ fit (Eq. (1)) for $T > 50$ K. The solid line is the best-fit curve to Eq. (2) (see text for details). (For interpretation of the references to color in this figure legend, the reader is referred to the web version of this article.)

of a bulk sample ($\alpha = 1.5$), but this result is consistent with theoretical calculations [23] and other results found for Fe-NPs [23–25]. The discrepancy with the bulk $T^{3/2}$ dependence could be attributed to both finite-size effects [25] and a lack of magnetic coordination at the surface [24], because the exponent α is size dependent but insensitive to the crystal structure [23]. On the other hand, the difference between the obtained value for the prefactor B and those reported in the literature [23,25,26], may be understood in terms of the co-existence of BCC and FCC crystal structures on Fe-AC sample (see Refs. [18,19]), as the prefactor B depends on the mean coordination number of the spins in the NP [23].

3.2. Mössbauer spectroscopy

The magnetism of the core/double-shell Fe-NPs on Fe-AC sample, may be affected by the magnetic character of the γ-Fe cores with mean size of ~10(2) nm. Mössbauer spectra at 4.2, 77 and 300 K provide information of the true magnetic order of the γ-Fe nuclei (see Fig. 2). Table 1 lists the refined values for the hyperfine fields (B_{HF}), quadrupole shift (2ε), isomer shift (δ) and, the line-width (Γ) together with the relative area of each component.

As it can be observed, the line-width of the central singlet contribution ascribed to the γ-Fe phase exhibits a broadening tendency within decreasing temperature. Prados et al. explained a similar feature on γ-Fe NPs inserted into carbon nanotubes due to a low temperature AFM transition [13]. However, they pro-

Table 1
Parameters deduced from the analysis of the Mössbauer spectra depicted in Fig. 2. B_{HF} is the hyperfine field; ε and δ are the quadrupole splitting and isomer shift, respectively, with reference to an α-Fe foil; Γ is the line-width (half width at half maximum). The proposed phase identification and their areas in relative percent are also given.

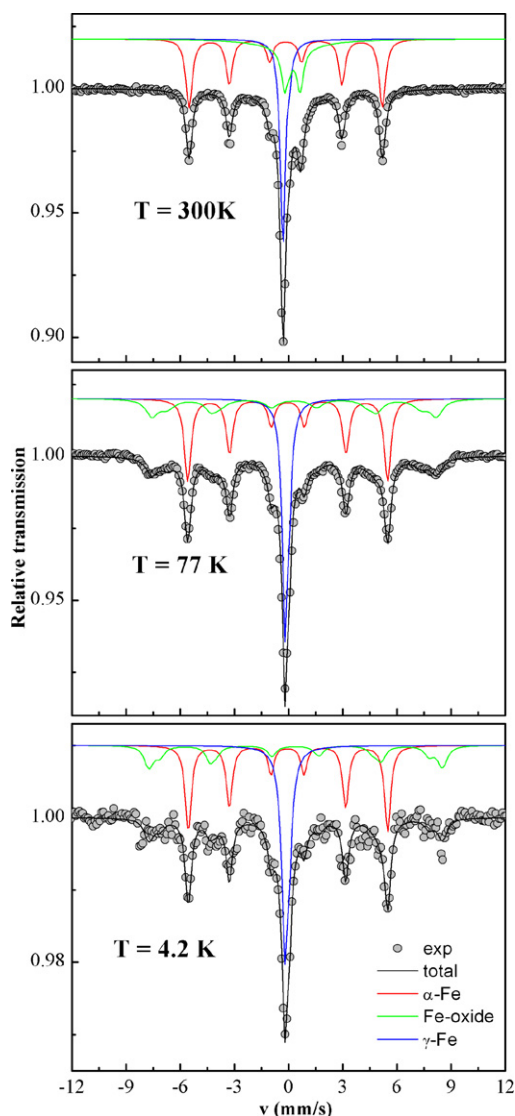| T (K)	Phase	B_{HF} (kOe)	δ (mm/s)	ε (mm/s)	Γ (mm/s)	Area (%)
	α-Fe	330	~0	0.01	0.21	43 (2)
300	Fe-oxide		0.38	0.75	0.22	14 (1)
			0.38		2.0	15 (1)
	γ-Fe		−0.10		0.18	28 (2)
	α-Fe	341	0.12	0	0.22	45 (2)
77	Fe-oxide	487	0.48	0	0.40	16 (1)
		434	0.48	0	0.50	11 (1)
	γ-Fe		0.02		0.19	28 (2)
	α-Fe	340	0.11	0.03	0.20	45 (2)
		513	0.57	0	0.18	2 (1)
4.2	Fe-oxide	500	0.55	0	0.30	15 (1)
		460	0.49	0	0.30	7 (1)
	γ-Fe		0.02		0.23	31 (2)

Fig. 2. ^{57}Fe Mössbauer spectra of the Fe NPs together with the fit obtained at 300, 77 and, 4.2 K. The black dots represent the experimental data and the solid lines the fitted spectra. Different subespectra corresponding to α-Fe (red), γ-Fe (blue) and Fe-oxides (green) phases have been considered. (For interpretation of the references to color in this figure legend, the reader is referred to the web version of this article.)

pose a morphology that consists of α-Fe NPs surrounded by an outer shell of γ-Fe phase. In our study, the FCC crystal structure is attained on the pyrolysis process at $900\,^{\circ}$C and retained on the subsequent slow cooling to room temperature on a controlled N_2 atmosphere. In addition, the bidimensional expansion needed for the transition from the metastable γ-Fe into stable α-Fe, seems to be more probable on the external surface of the Fe-NPs [14].

4. Discussion

Taking into account the phase percentages estimated from Mössbauer spectroscopy (that are in excellent agreement with the analysis of room temperature XAS results, see Ref. [19]) [α-Fe (45%), γ-Fe (31%) and γ-Fe$_2$O$_3$ (24%)] (see Table 1), and assuming: (i) a negligible contribution of γ-Fe phase; (ii) $M_s \approx 222$ emu/g for the low temperature α-Fe phase (because its hyperfine field value matches with that of pure bulk α-Fe, $B_{HF} = 330$ kOe); (iii)

a value of M_s (γ-Fe$_2$O$_3$) ≈ 80 emu/g, we should expect roughly 120 emu/g for the M_s of the sample (normalized to the total amount of Fe). However, the relative percentage of carbon in the Fe-AC sample is above 80 wt.%, therefore the obtained value for the net magnetization of the sample, 13.3 emu/g (see inset Fig. 1), must be normalized to the real amount of Fe (only 16.8 wt.%, see ref. [17]), giving rise to an experimental value $M_s \approx 80$ emu/g, lower than expected (120 emu/g, see above). This discrepancy can be attributed to two main reasons. First of all, the M_s of the Fe oxides decreases drastically at the nanoscale [21]. Secondly, competing FM/AFM interactions and spin disorder between Fe atoms must exist at the interface between the γ-Fe core and the inner α-Fe shell due to the change from FCC to BCC crystal structures. A simple estimation of the boundary width, d_{BW}, taking into account that only 2/3 of the expected M_s is obtained, gives a reasonable value of $d_{BW} \approx 0.7$ nm, which roughly corresponds to two γ-Fe or 2.5 α-Fe unit cells.

5. Conclusions

In summary, we report the challenge of synthesizing stable γ-Fe phase on Fe-NPs with nano-onion-like morphology of core (γ-Fe)/double shell (α-Fe/maghemite). The Fe-NPs exhibit a reduced saturation magnetization value likely due to the disordered spins in competing FM/AFM interactions at the BCC-FCC interface. Low temperature Mössbauer spectrum reveals a broadening of the line-width contribution of the γ-Fe phase that may suggest the existence of AFM γ-Fe. Further experiments are required to elucidate the specific effects derived from the uncompensated sublattices on AFM NPs.

References

[1] D. Zhang, et al., Nanoscale 2 (2010) 917–919.
[2] S.R. Rudge, et al., Biomaterials 21 (2000) 1411–1420.
[3] D.L. Huber, Small 1 (2005) 482–501.
[4] J. Nogues, et al., Phys. Rep. Rev. Sec. Phys. Lett. 422 (2005) 65–117.
[5] P. Gorria, et al., Carbon 44 (2006) 1954–1957.
[6] P. Gorria, et al., Phys. Status Solidi RRL 3 (2009) 4–6.
[7] M.P. Fernandez-García, et al., Phys. Chem. Chem. Phys. 13 (2011) 927–932.
[8] R. Sergiienko, et al., Carbon 47 (2009) 1056–1065.
[9] A. Taylor, et al., J. Nanopart. Res. 12 (2010) 513–519.
[10] T. Enz, et al., J. Appl. Phys. 99 (2006) 044306.
[11] J.F. Geng, et al., Chem. Commun. (2004) 2442–2443.
[12] K. Haneda, et al., Phys. Rev. B 46 (1992) 13832–13837.
[13] C. Prados, et al., Phys. Rev. B 65 (2002) 113405.
[14] V. Pichot, et al., Appl. Phys. Lett. 85 (2004) 473–475.
[15] P. Gorria, et al., Phys. Rev. B 80 (2009) 064421.
[16] P. Gorria, et al., Phys. Status Solidi RRL 3 (2009) 115–117.
[17] M.P. Fernandez, et al., J. Non Cryst. Solids 354 (2008) 5219–5221.
[18] M.P. Fernández, et al., J. Magn. Magn. Mater. 322 (2010) 1300–1303.
[19] M.P. Fernandez-García, et al., Phys. Rev. B 81 (2010) 094418.
[20] D. Fiorani, et al., J. Phys. Condens. Matter 19 (2007).
[21] R.C. O'Handley, Modern Magnetic Materials. Principles and Applications, John Wiley & Sons, Inc., New York, 2000.
[22] C. Kittel, Introduction to Solid State Theory, Wiley, New York, 1971.
[23] P.V. Hendriksen, et al., Phys. Rev. B 48 (1993) 7259–7273.
[24] S. Linderoth, et al., J. Magn. Magn. Mater. 124 (1993) 269–276.
[25] L.M. Lacroix, et al., J. Appl. Phys. 103 (2008) 07D521.
[26] M. Wilke, et al., Am. Miner. 86 (2001) 714–730.